ACS OMEGA

Open Access

http://pubs.acs.org/journal/acsodf

Article

Adding Granular Activated Carbon and Zerovalent Iron to the High-Solid Anaerobic Digestion System of the Organic Fraction of Municipal Solid Waste: Anaerobic Digestion Performance and Microbial Community Analysis

Hongfei Zhang, Hairong Yuan,* Xiaoyu Zuo, Liang Zhang, and Xiujin Li*

Cite This: *ACS Omega* 2024, 9, 3401−3411

Read Online

ACCESS | Metrics & More | Article Recommendations

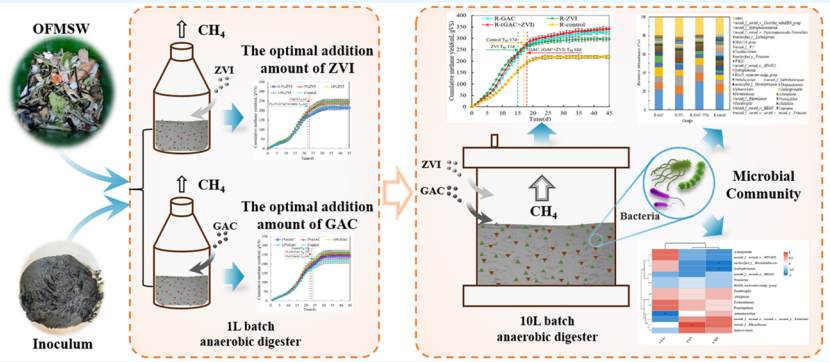

ABSTRACT: Anaerobic digestion (AD) performance and microbial dynamics were investigated in a high-solid anaerobic digestion (HSAD) system of the organic fraction of municipal solid waste (OFMSW). 1, 5, 10, and 15% (w/w, dry weight of the OFMSW) of granular activated carbon (GAC) and zerovalent iron (ZVI) were added to the HSAD system. The results showed that adding ZVI and GAC can improve the methane yield of the OFMSW. Notably, R-(GAC + ZVI) exhibited the highest cumulative methane yield of 343.0 mL/gVS, which was 57.1% higher than that of the R-control. At the genus level, the dominant bacteria included norank_f__norank_o__*MBA03*, norank_f__norank_o__norank_c__norank_p__*Firmicutes*, *Fastidiosipila*, norank_f__*Rikenellaceae*, and *Sphaerochaeta*, while *Methanoculleus*, *Methanobacterium*, and *Methanosarcina* were the dominant archaea. The highest relative abundance of norank_f__norank_o__norank_c__norank_p__*Firmicutes* was 30.8% for the R-(GAC + ZVI), which was 71.4% higher than that of the R-control. The relative abundance of *Methanoculleus* and *Methanobacterium for* the R-(GAC + ZVI) and the R-control group accounted for 79.0 and 90.8% of the total archaeal abundance, respectively. Additionally, the relative abundance of *Methanosarcina* was 10.6% for R-(GAC + ZVI), which was higher than that of the R-control (1.1%). After the addition of GAC and ZVI, the electron transfer capacity of the HSAD system was enhanced, resulting in promoted methane production. Thus, the simultaneous addition of GAC and ZVI to the HSAD system can be an effective strategy to promote the cumulative methane yield of the OFMSW.

1. INTRODUCTION

In response to the global energy crisis and the need for meeting climate targets, there is a growing interest in employing carbon-neutral techniques to convert waste into clean and renewable energy sources. Anaerobic digestion (AD) is considered one of the most effective carbon neutralization techniques for harnessing energy from waste.[1] According to data from the Ministry of Ecology and Environment of the People's Republic of China, China generated about 2.4 billion tons of municipal solid waste in 2022,[2] with the organic fraction of municipal solid waste (OFMSW) comprising 40−68% of the total municipal solid waste.[3] The OFMSW is a complex mixture primarily consisting of kitchen waste, food waste, yard waste, paper, fallen leaves, and other organic wastes.[4] The OFMSW exhibits a high moisture content, a low carbon-to-nitrogen ratio, and a high volatile solid content, making it more suitable for AD to produce energy compared to landfilling and biofertilizer techniques.[4]

Received: September 5, 2023
Revised: December 15, 2023
Accepted: December 22, 2023
Published: January 12, 2024

For the OFMSW, dry or solid-state AD (with a total solid content of >20%) is more advantageous owing to its small digestion volume, high total solid content, less wastewater problem, and increased methane production potential.[5] However, the high total solid content can lead to the accumulation of volatile fatty acids and the inhibition of ammonia nitrogen because of reduced mass transfer during the OFMSW AD process. Therefore, improving the mass transfer effect of dry or solid-state AD systems is necessary to enhance the AD efficiency. Studies have shown that the addition of conductive materials, such as carbon-based and iron-based materials, can stimulate interspecies electron transfer within AD systems and improve the methane yield.[6] Generally, carbon-based materials include graphene, biochar, granular and powder activated carbon, carbon cloth, and carbon nanotubes, while iron-based materials involve magnetite, zerovalent iron (ZVI), hematite, and stainless steel.[7]

Wang et al.[1] investigated different conductive materials in a dry AD system to enhance methane production, revealing that all conductive materials could promote methane production. However, variations in the experimental conditions resulted in considerable differences in methane production. Similarly, Kutlar et al.[8] investigated 10 different carbon-based materials and discovered that granular activated carbon (GAC), biochar, and carbon cloth were the most frequently utilized materials. Compared to biochar, GAC has a higher electrical conductivity owing to the characteristics of GAC, such as its porosity, expansive surface area, and aromatic structure, via which microbes facilitate electron transport through GAC.[6] According to reports,[8] the role of GAC is mainly in improving AD performance. The introduction of GAC led to a methane yield increase 1.17−17.85-fold higher than that of the control group across different substrates. In addition, the GAC dosage used was 0.03 g/mL−50 g/L, along with a GAC particle diameter of 0.8−2.4 mm.[9] However, the optimal amount of GAC addition exhibited significant variability among different substrates. For instance, Dastyar et al.[10] put 15 $g/L_{percolate}$ powdered activated carbon into a high-solid anaerobic digestion (HSAD) system, resulting in a 17% increase in cumulative biomethane yield for the OFMSW compared to that of the control. Tiwari et al.[11] reported that the highest biogas yield from wheat husk was achieved with the addition of 20 g/L GAC, while the total biogas yield decreased as the GAC dosage increased from 30 to 50 g/L compared to that of the control group. Similarly, during the dry AD process of swine manure, the addition of GAC under the mesophilic conditions increased the methane production of the AD system and shortened the lag phase.[12] Interestingly, when 50 g/L GAC was added to commercial dog food (similar to the OFMSW in composition), the highest cumulative methane production was obtained.[13] Nonetheless, some researchers reported no difference in cumulative methane production between the GAC-added group and the control group for seed biomass from wastewater treatment plants.[14] In contrast, in some cases, such as fat, oil, and grease (FOG) digestion, the addition of GAC resulted in a 10−57% reduction in methane production compared to that of the control group.[15] Thus, the optimal addition amount of GAC remains unclear, reflecting the variability in outcomes across different substrates and experimental conditions.

Iron-based materials have been widely employed to promote methanogenesis compared to carbon-based materials.[7] The range of the added amounts and subsequent methane yield enhancements of different substrates resulting from the incorporation of iron-based materials are 10−27 g/L and 1.07−18 times higher than those observed in the control group, respectively.[9] Wang et al.[16] compared the effect of ZVI, magnetite, and ferric oxide in different amounts on the AD performance of food waste, revealing the highest cumulative methane production from food waste for the ZVI group, with an added amount of 5 g/L. Liang et al.[17] reported that codigestion processes involving food waste and sewage sludge, the introduction of 10 g/L ZVI, biochar, and Fe_3O_4, resulted in the ZVI (10 g/L) group exhibiting methane yields 1.24 times higher than that of the magnetite group. However, Kassab et al.[18] found contrasting results in codigestion with food waste and waste activated sludge at the nanoscale level. The methane production of the magnetite (25 g/L) group was 50% higher than that with the addition of ZVI (25 g/L) group. Additionally, Zhao et al.[19] suggested that the addition of ZVI (10 g/L) had a minor effect on the hydrolysis and acidification of waste activated sludge. In contrast, methane production increased by 70% for the ZVI group and decreased by 22% for the Fe_3O_4 group compared with the control group. Sulfide nanoscale ZVI was found to considerably promote the methane yield from food waste (18 times);[20] however, the cost of nanoscale ZVI proved to be high compared to ZVI and Fe_3O_4. Considering HSAD systems with the OFMSW, the additions of ZVI and nanoscale ZVI at 0.4−0.8 g/gVS in a 20 gVS/L substrate resulted in the highest methane yield of 330.6 mL/gVS observed in the ZVI (0.7 g/gVS) group.[21] Therefore, there is a lack of consistency in the optimal addition amounts of iron-based materials and there are few related studies on the dry or solid-state AD system, highlighting the need for further research in this area.

The primary mechanism by which conductive materials improve AD performance involves facilitating direct electron transfer from certain bacteria to archaea through these conductive materials. This process enables the syntrophic metabolisms of microorganisms, a phenomenon known as direct interspecies electron transfer (DIET).[9] In AD systems where conductive materials are introduced, specific bacterial species, such as *Geobacter*, *Sporanaerobacter*, *Geobacteraceae*, *Clostridium*, *Sphaerochaeta*, *Defluviitoga*, *Thermovirga*, and *Cloacibacillus*, have been frequently identified.[22] Conversely, archaea mainly comprises *Methanosarcina*, *Methanosaeta*, *Methanoculleus*, *Methanobacterium*, and *Methanospirillum* in the AD system, along with added conductive materials.[17] Notably, some researchers have focused their attention on the microbial community in wet AD processes involving food waste and the OFMSW with conductive materials, but research on dry or solid-state AD for the OFMSW is considerably low.

Herein, the OFMSW was used as the experimental feedstock and ZVI and GAC were used as conductive materials in the HSAD system. The main objective of this study is to (1) investigate the effect of ZVI and GAC addition amounts on the HSAD performance of the OFMSW, (2) analyze the effect of addition strategies on HSAD performance, and (3) compare the microbial community characteristics of OFMSW after addition of GAC and ZVI with the HSAD system.

2. MATERIALS AND METHODS

2.1. OFMSW and Inoculum. The OFMSW used in this study was sourced from the garbage collection station of the Sakura-Yuan community in Chaoyang District, Beijing, China. The components of the OFMSW mainly contained food waste, vegetable and fruit waste, and a minor presence of garden

https://doi.org/10.1021/acsomega.3c06722
ACS Omega 2024, 9, 3401−3411

waste. Nondegradable items such as bones and plastics were removed. Subsequently, the OFMSW was processed into particles of <5 mm using a food pulverizer and stored in a refrigerator until needed. The inoculum for the study was collected from a dry AD system handling food waste at the Dongcun Comprehensive Treatment Plant in Beijing, China. The characteristics of the OFMSW and inoculum are listed in Table 1.

Table 1. Basic Properties of Raw Materials (Wet Basis)

items	OFMSW	inoculum
total solid (TS, %)	28.3	25.1
volatile solid (VS, %)	20.2	8.9
VS/TS (%)	71.4	35.5
C/N	11.6	10.6
pH	5.62	8.59
total ammonia nitrogen (TAN, mg/L)	620	2240
alkalinity (mg $CaCO_3$/L)	730	11,900

2.2. Experimental Methods. The batch AD experiments included two groups: the first group focused on determining the optimal addition amounts of GAC and ZVI, while the second group aimed to compare the effects of different addition strategies employing GAC and ZVI on AD performance. The experiments of the GAC and ZVI addition amount were performed in a 1 L blue cap bottle. The TS addition amount of the OFMSW for each bottle was 40 g of TS. The addition amounts of GAC and ZVI accounted for 1, 5, 10, and 15% (w/w) dry weight (TS) of the OFMSW. During the experiment, each bottle was manually shaken twice a day for 5 min each time to ensure uniform mixing. Each experimental group was conducted in triplicate, and the results were calculated as the mean of the triplicate. For the second group of experiments involving GAC and ZVI addition, a 10 L batch anaerobic digester with a leachate circulation system was employed. The TS addition amount of the OFMSW for each anaerobic digester was 200 g of TS. The addition amounts of GAC and ZVI were categorized into four groups: unadded group (0%), 5%GAC, 5%ZVI, and 5%GAC + 5%ZVI (w/w) dry weight of OFMSW. These groups were denoted as R-control, R-GAC, R-ZVI, and R-(GAC + ZVI), respectively. Owing to the impracticality of manual shaking within the 10 L AD, efforts were made to ensure even moisture distribution of raw materials in the reactor. The leachate from the bottom of the reactor was collected daily and then sprayed from the top of the reactor to the surface of the raw material at regular intervals daily. Properties of the leachate, including pH, TAN concentration, and VFAs, were measured every 5 days. Three parallel samples were taken for each test parameter, and the mean value of the triplicate was used for test results. Throughout both sets of experiments, a single inoculum and a single OFMSW without GAC and ZVI were used as the control group to offset the effect of the inoculum and compare the effect of GAC and ZVI addition, respectively. The ratio of the inoculum to the OFMSW (TS) was maintained at 3:1, and the TS content in each test system was set at 25%. The AD temperature and AD time were set to 35 ± 1 °C and 45 days according to previous studies' results, respectively.[23]

2.3. Analytical Methods. Daily biogas production and gas components were recorded through a water displacement method and gas chromatograph (SP-2100, Zhongkehuijie Corporation, Beijing, China) with a TDX-01 column and a thermal conductivity detector. TS and VS were measured following the standard methods. Total nitrogen and total carbon contents, pH, and TAN were detected with an elemental analyzer (Vario EL/micro cube elemental analyzer, Germany), pH meter (Thermo Electron, Waltham, MA), and HANNA environmental testing photometer (HI83206, China), respectively. Free ammonia nitrogen (FAN) was calculated using eq 1 according to the values for TAN, pH, and solution temperature.[24] VFAs were analyzed by using gas chromatography (GC-2014, Shimadzu, Japan) equipped with a flame ionization detector.

$$\mathrm{FAN} = \mathrm{TAN} \times \left(1 + \frac{10^{-\mathrm{pH}}}{10^{-\left(0.09018 + \frac{2729.92}{T(\mathrm{K})}\right)}}\right)^{-1} \quad (1)$$

where FAN, TAN, and T(K) were the free ammonia nitrogen concentration (mg/L), total ammonia nitrogen concentration (mg/L), and Kelvin temperature (K), respectively.

2.4. Kinetic Analysis. The modified Gompertz (eq 2) and logistic (eq 3) models were used to fit the methane production of the OFMSW for different addition amounts of GAC and ZVI, according to Guan et al.'s approach.[25]

$$P(t) = P_\mathrm{m} \exp\left\{-\exp\left[\frac{R_\mathrm{m} e}{P_\mathrm{m}}(\lambda - t) + 1\right]\right\} \quad (2)$$

$$P(t) = \frac{P_\mathrm{m}}{1 + \exp[-k(t - \lambda)]} \quad (3)$$

where $P(t)$, P_m, and R_m were the simulated methane yield at time t (mL/gVS), the maximum methane potential at the end of AD (mL/gVS), and the maximum methane production rate (mL/gVS·d), respectively. The functions λ, t, and k were the lag phase time (d), AD time (d), and methane production rate constant (d^{-1}), respectively. The constant e is 2.71828. The domain of the two models was ≥0.

2.5. Microbial Community Analysis. Microbial samples were collected from the second-group experiments after the end of 45 days, AD 45, and were named R-control, R-GAC, R-ZVI, and R-(GAC + ZVI). Four samples were analyzed by Shanghai Meiji Biopharmaceutical Technology Co., Ltd. Microbial DNA from the samples was extracted using the FastDNA Spin Kit (MP Biomedicals) following the manufacturer's protocol. The primers 338F(5′-ACTCCTACGGGAGGCAGCAG-3′) and 806R(5′-GGACTACHVGGGTWTCTAAT3′) were used to recognize bacteria, while the primers 524F_10_ext (5′-TGYCAGCCGCCGCGGTAA-3′) and arch 958R (5′-YCCGGCGTTGAVTCCAATT-3′) were used to identify archaea. High-throughput 16S rRNA gene sequencing was performed using the Illumina MiSeq platform (Illumina Company), and subsequent microbial data were analyzed through means of the Major BioCloud online platform.

2.6. Statistical Analysis. Microsoft Excel 2022 and Origin 2021 were used to estimate standard deviations, statistical differences, and nonlinear fitting of the model. Pearson correlation analysis was performed via the Major BioCloud platform. Symbols *, **, and *** represent the statistically significant values $P \leq 0.05$, 0.01, and 0.001, respectively.

https://doi.org/10.1021/acsomega.3c06722
ACS Omega 2024, 9, 3401−3411

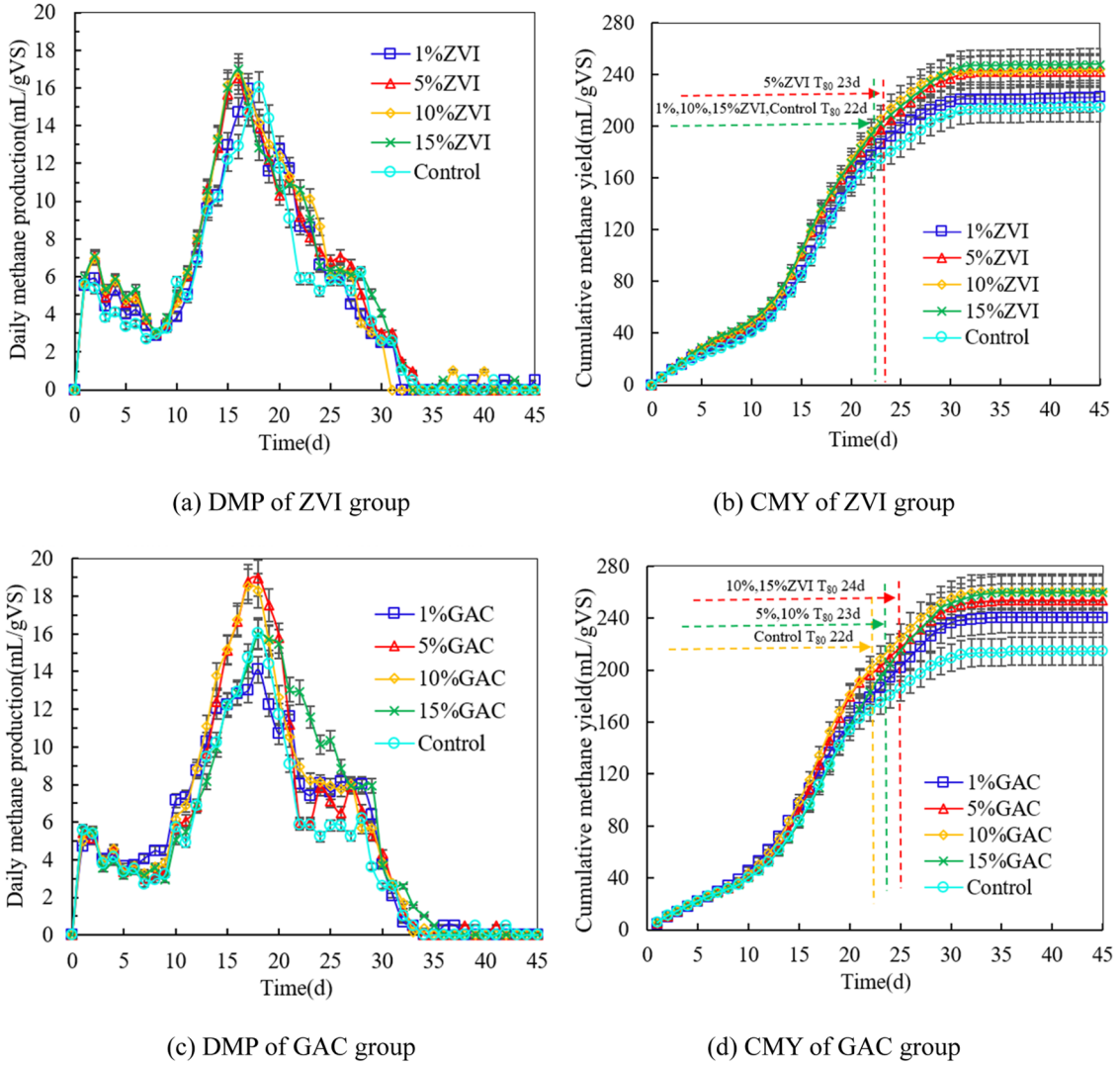

Figure 1. Methane production of different experiment groups.

3. RESULTS AND DISCUSSION

3.1. Effect of the Addition Amount of ZVI and GAC on the HSAD Performance of the OFMSW. *3.1.1. Methane Production.* The daily methane production (DMP) exhibited a consistent trend in different experimental groups with varying addition amounts of ZVI and GAC (Figure 1(a),(c)). All experiment groups displayed three distinct DMP peaks. The DMP peak values for the ZVI-added groups appeared at 5.6−7.1, 15.9−17.0, and 6.0−7.1 mL/gVS on 1−2, 16−17, and 26−28 days, respectively. The time of the DMP peak value appearing for the GAC group was similar to that for ZVI-added groups. For GAC groups, the maximum DMP values were 14.1, 19.0, 18.5, and 16.0 mL/gVS for 1%GAC, 5%GAC, 10% GAC, and 15%GAC, respectively, which were 0%−18.2% higher than that of the control group. The highest DMP of 5% GAC (19.0 mL/gVS) was 11.9−19.2% higher than those of ZVI-added groups. This is attributed to the special porous surface properties of GAC, allowing it to adsorb inhibitory materials, such as VFAs and heavy metals, while promoting DIET.[7] The time of the maximum DMP peak value for the ZVI groups appeared on the 16th−17th days, which was 1−2 days compared to the GAC groups.

The cumulative methane yields (CMYs) of different addition groups are shown in Figure 1(b),1(d). CMY exhibited an upward trend for different groups in the first 30 days; then, a slow change trend appeared from 30 to 45 days. CMYs of ZVI and GAC groups were 222.6−247.8 and 240.5−260.6 mL/gVS, which were 3.8−15.5 and 12.1−21.4% higher than that of the control group, respectively. Wang et al.[16] found that after the addition of 5 g/L ZVI, cumulative methane production of food waste increased by 8.5% higher than that of the control. Similarly, a CMY with an increasing rate of 17% was achieved for HSAD of the OFMSW with 15 g/L powdered activated carbon, compared to the control.[10] Simultaneously, a CMY improvement rate of 27% was found in the AD system of wheat husk with the addition of 20 g/L GAC.[11] The CMY of the GAC groups was 5.1−17.0% higher than those of the ZVI groups. Conversely, a recent study showed that the methane improvement capability of iron-based materials was better than that of carbon-based materials in the wet AD system of codigestion with food waste and sewage sludge.[17] This difference may be attributed to two possible reasons: one is the differences in physicochemical properties and role mechanism of carbon-based materials and iron-based materials in the AD system;[6] the other is the complex composition of the

https://doi.org/10.1021/acsomega.3c06722
ACS Omega 2024, 9, 3401−3411

Table 2. Estimated Parameters of the Modified Gompertz and Logistic Models

		modified Gompertz model				logistic model			
groups	experimental values (mL/gVS)	P_m (mL/gVS)	R_m (mL/gVS·d)	λ (d)	R^2	P_m (mL/gVS)	R_m (mL/gVS·d)	λ (d)	R^2
1%GAC	240.5	280.5	11.5	6.1	0.996	251.1	18.6	12.4	0.999
5%GAC	253.5	276.6	13.2	7.3	0.991	253.0	21.2	12.8	0.997
10%GAC	260.6	292.5	13.9	7.1	0.994	268.0	22.2	12.7	0.998
15%GAC	259.4	312.9	12.6	7.6	0.993	274.3	20.8	13.9	0.999
1%ZVI	222.6	254.5	11.3	6.2	0.990	230.9	18.4	12.1	0.997
5%ZVI	242.5	278.3	11.8	5.7	0.992	251.1	19.2	11.8	0.998
10%ZVI	244.0	278.1	12.5	6.0	0.990	253.7	20.3	11.9	0.997
15%ZVI	247.8	285.6	11.8	5.5	0.993	256.9	19.3	11.8	0.998
control	214.6	241.8	10.9	6.4	0.991	220.1	17.7	12.2	0.998
R-GAC	327.6	324.9	19.5	3.3	0.998	318.0	29.1	7.9	0.997
R-ZVI	296.9	296.5	21.2	2.2	0.999	292.6	30.9	6.1	0.997
R-(GAC + ZVI)	343.0	337.1	20.9	3.1	0.998	330.4	31.1	7.6	0.996
R-control	218.3	222.7	15.6	4.0	0.993	219.3	23.0	8.0	0.999

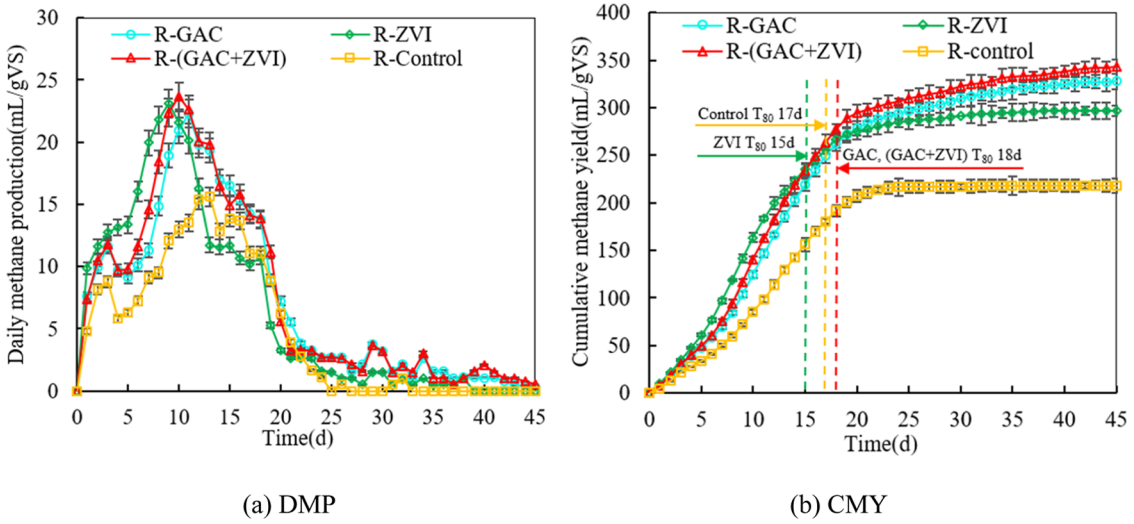

(a) DMP (b) CMY

Figure 2. Methane production of different addition materials of ZVI and GAC.

OFMSW and restricted mass transfer in the HSAD system.[16] The maximum CMY was 247.8 and 260.6 mL/gVS for 15% ZVI and 10%GAC, respectively. Increasing the addition amount of ZVI and GAC from 5 to 15% did not produce significant differences in the CMY of the ZVI groups ($P > 0.05$) and the GAC groups ($P > 0.05$). Therefore, considering the cost of the addition material, 5% ZVI and 5% GAC were recommended as the optimal addition amount.

To assess the digestion efficiency of the AD system, 80% of total methane production (T_{80}) was used. The T_{80} of the ZVI groups was 22−23 days, which was 1−2 days shorter than those of the GAC groups (Figure 1(d)). However, there were no obvious differences in T_{80} between the different ZVI and GAC addition groups compared with that of the control (22 days). The phenomenon of shortening AD period did not appear in this study after addition of conductive materials.

3.1.2. Kinetic Analysis. The fitting kinetic parameters of the modified Gompertz and logistic models for different experimental groups are shown in Table 2. The differences between the experimentally measured methane yield and the predicted P_m values (Table 2) were 9.1−20.6 and 0.2−5.4% for the modified Gompertz and logistic models, respectively. Notably, the P_m values of the logistic model and the experiment values were very close, indicating that the logistic model is more favorable in simulating the CMY of experimental data compared to the modified Gompertz model. The R_m values for the modified Gompertz and Logistic models were 10.9−13.9 and 17.7−22.2 mL/gVS·d, respectively. The R_m values for the logistic model closely aligned with the actual DMP peak values of 15.9 × 17.0 and 14.1 × 19.0 mL/gVS for ZVI and GAC addition groups, respectively. The lag phase time of AD (λ) implies the time required for the microbial community to adapt in the digester.[26] The λ values of the modified Gompertz and logistic models for the ZVI and GAC addition groups closely resembled those of the control group, indicating that the addition of ZVI or GAC did not improve the AD speed in the HSAD system, which is consistent with the experimental results. The R^2 values for the modified Gompertz and Logistic models were 0.990−0.996 and 0.997−0.999, respectively. The R^2 for the logistic models approached 1, indicating that the logistic model can precisely fit the HSAD process.

3.2. Effect of the Addition Strategy of ZVI and GAC on the HSAD Performance of the OFMSW. *3.2.1. Methane Production.* Similar to the changing trend observed in different ZVI and GAC addition experiment groups, DMP of R-GAC, R-ZVI, and R-(GAC + ZVI) also appeared with 2 and 3 peak values (Figure 2(a)). The highest DMP peak value was 23.6

https://doi.org/10.1021/acsomega.3c06722
ACS Omega 2024, 9, 3401−3411

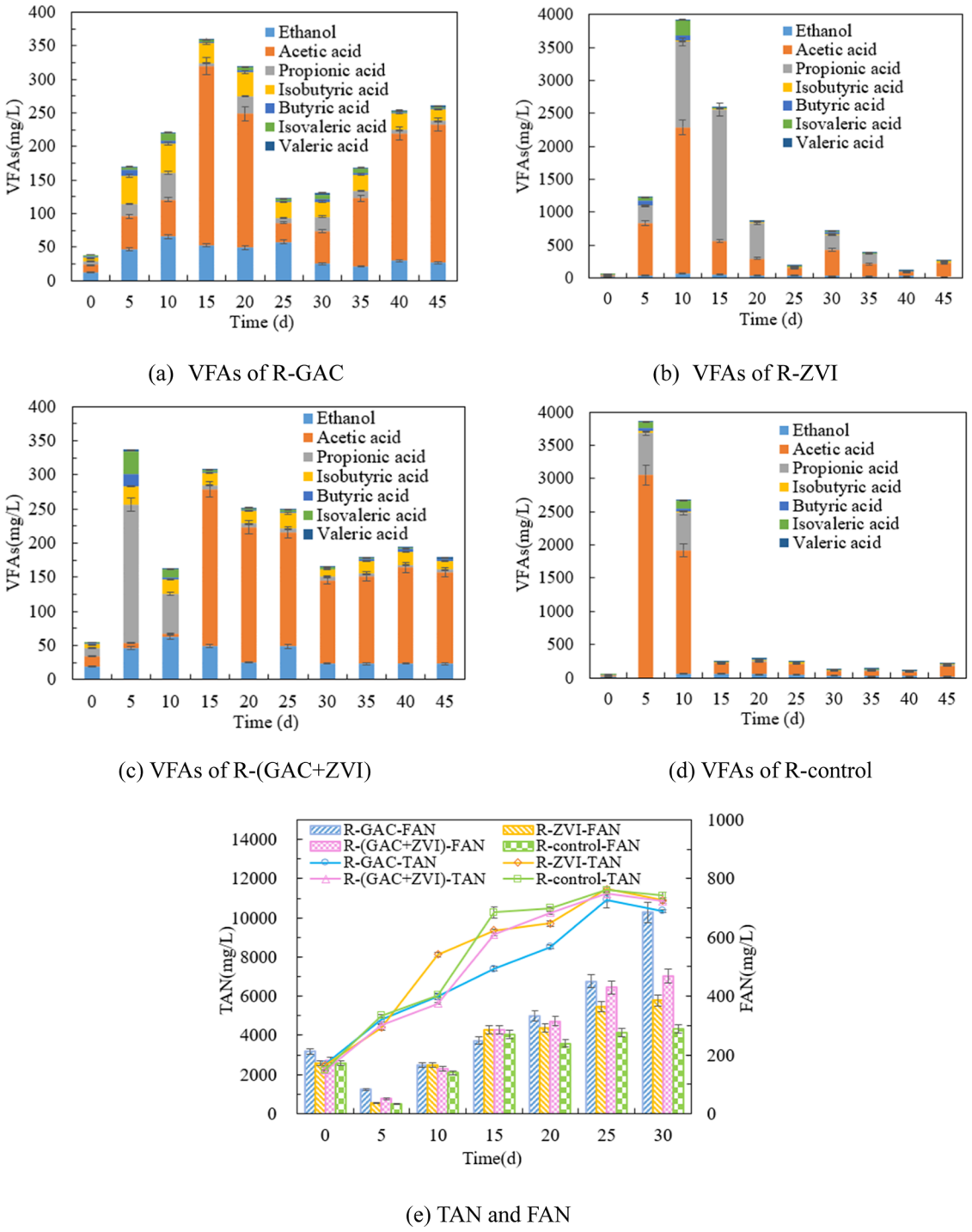

Figure 3. Changes of VFAs, TAN, and FAN in the leachate.

mL/gVS in R-(GAC + ZVI) groups on day 10, which was 2.3, 6.1, and 51.5% higher than those of the R-ZVI, R-GAC, and R-control groups, respectively. The time of the highest DMP peak value appearing for R-ZVI was on day 9, which was 1, 2, and 4 days earlier than those of the R-ZVI, R-GAC, and R-control groups, respectively.

In the first 20 days, the CMY of R-GAC, R-ZVI, and R-(GAC + ZVI) rapidly increased, and then, a slowly changing trend was observed from 21 to 45 days (Figure 2(b)). The CMYs of the R-GAC, R-ZVI, and R-(GAC + ZVI) groups were 327.6, 296.9, and 343.0 mL/gVS, which were 50.0, 36.05, and 19.% higher than that of the R-control group, respectively. The CMYs of the control (the first group-1L) and R-control (the other group-10L) were close, with values of 214.6 and 218.3 mL/gVS, respectively, and were showing no considerable difference. However, the CMYs of R-GAC and R-ZVI were 29.2 and 22.4% higher than those of the 5%GAC and 5% ZVI groups, respectively, indicating the positive role of recycled leachate in improving the CMY. The maximum CMY of 343.0 mL/gVS was obtained in the R-(GAC + ZVI) group, which was 15.5 and 4.7% higher than that of R-ZVI and R-GAC, respectively. Dai et al.[27] found that a 11.0% improvement in methane production of pharmaceutical wastewater after addition of ZVI and GAC. Similarly, 5 g/L

https://doi.org/10.1021/acsomega.3c06722
ACS Omega 2024, 9, 3401−3411

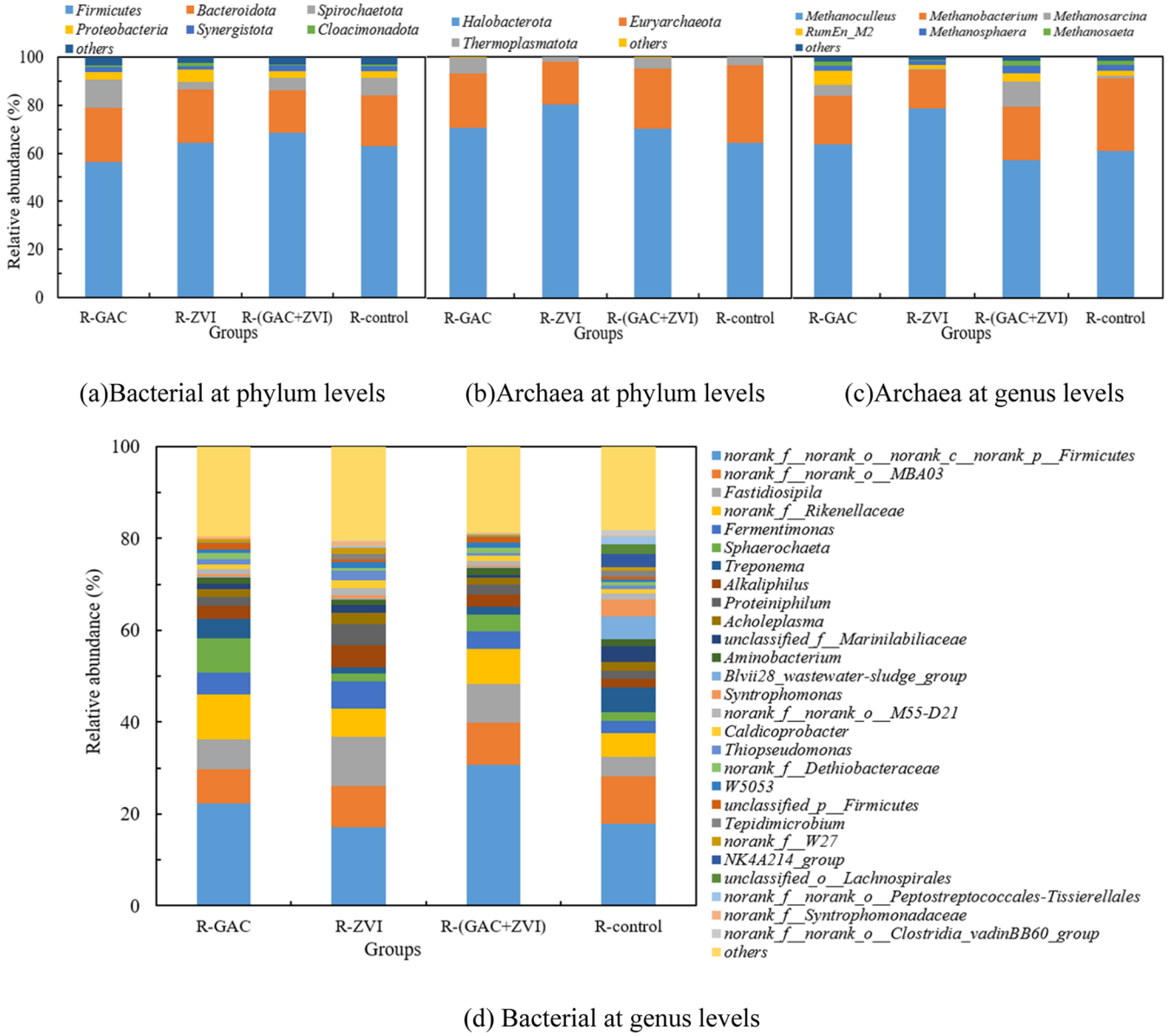

Figure 4. Relative abundances of bacteria and archaea at phylum and genus levels.

ZVI and 5 g/L activated carbon were added to the wet AD system of food waste, resulting in a 35.0% increase for the CMY of food waste.[28] Furthermore, after biochar and ZVI were added to the AD system of food waste, the CMY of food waste increased by 19.4% compared with the biochar addition group.[29] These findings describe that GAC has excellent physicochemical characteristics, including its specific surface area and particle size as well as the potential of ZVI to provide iron as a coenzyme and alternative electron donor, thereby enhancing the growth of H_2-utilizing microorganisms to improve methane production.[30] Therefore, the simultaneous addition of GAC and ZVI in the HSAD system proves to be effective in promoting the CMY of the OFMSW.

T_{80} of R-GAC, R-ZVI, and R-(GAC + ZVI) was 18, 15, and 18 days, respectively, while it was 17 days (Figure 2(b)). T_{80} of R-ZVI was shortened 2, 3, and 3 days compared with the R-control, R-GAC, and R-(GAC + ZVI), respectively. This indicated that adding ZVI in the HSAD of the OFMSW shortens the AD period and improves AD efficiency. This phenomenon aligns with the result of Alam et al. that adding conductive materials can shorten the AD period in the AD process.[7]

3.2.2. Kinetic Analysis. The kinetic parameters of R-GAC, R-ZVI, R-(GAC + ZVI), and R-control are listed in Table 2, according to the modified Gompertz and logistic models. P_m values of the modified Gompertz and Logistic models were 222.7−337.1 and 219.3−330.4 mL/gVS, respectively. The differences between P_m and the experimentally measured methane yields were 0.13−2.0 and 0.5−3.8% for the modified Gompertz and logistic models, respectively. The R_m values of the modified Gompertz and logistic models were 15.6−21.2 and 23.0−31.1 mL/gVS·d, respectively, which were very close to the actual DMP peak values of 15.6−23.6 mL/gVS. The R^2 values of the modified Gompertz were 0.993−0.999, indicating a closer fit to the experimental data compared to the logistic models. These results showed that the modified Gompertz model is more favorable in simulating the CMY of experiment data than the logistic model. This fully demonstrated that the

https://doi.org/10.1021/acsomega.3c06722
ACS Omega 2024, 9, 3401−3411

modified Gompertz model can adapt to the more complex AD.[31]

3.2.3. VFAs and TAN in the Leachate. The leachate from the AD system of the OFMSW can indirectly reflect the properties of the AD system. After the addition of GAC and ZVI, the VFA concentration of the AD system for the OFMSW considerably changed (Figure 3). During the whole AD process, VFA concentrations in R-GAC and R-(GAC + ZVI) were 38.1−360.3 and 54.8−308.6 mg/L, respectively. The highest VFA concentrations in R-GAC and R-(GAC + ZVI) were 90.7 and 91.3% lower than that in the R-control, respectively. VFA concentration in R-ZVI followed a trend similar to that of the R-control. The highest VFA concentration in R-ZVI (3929.3 mg/L) appeared on day 10, which was 5 days later than those of the R-control and R-(GAC + ZVI). The highest VFA concentration in R-GAC was observed on day 15, which was 5 and 10 days later than those of the R-ZVI and R-control, respectively, indicating that GAC and ZVI addition can alleviate and delay acidification. This result was consistent with the result of Ryue et al.[32] that adding GAC reduces VFA concentration in wet AD systems. A similar trend was observed when powdered activated carbon was added to the OFMSW in the HSAD system.[10] According to the literature reports, the methanogen activity of the AD system will be inhibited when the VFA concentration exceeds 6000 mg/L.[33] In all experimental groups, the range of VFA concentrations ranged from 38.1 to 3929.3 mg/L, which did not extend beyond this inhibition range; thus, the AD system was not inhibited by VFAs. In the AD system, the composition of VFAs usually plays an important role. The concentration of acetic acid was 11.3−266.9, 12.5−2224.4, 7.4−229.8, and 11.3−3057.4 mg/L for R-GAC, R-ZVI, R-(GAC + ZVI), and R-control, accounting for 23.5−74.1, 19.9−64.2, 2.2−78.7, and 22.6−79.1% of total VFAs, respectively. The propionic acid concentration in R-ZVI was 1988.5 mg/L on day 15, accounting for 76.9% of total VFAs. Compared with acetic acid, the slow conversion rate of propionic acid during methanation could inhibit the activity of methanogens owing to excessive propionic acid.[22] This is probably the main reason for the lower CMY in R-ZVI than that in R-GAC and R-(GAC + ZVI).

During the experiment, the TAN concentration gradually increased from 2210.0 to 11,420 mg/L (Figure 3(e)). The TAN concentrations in the GAC and ZVI addition groups were all lower than that in the R-control, except for R-ZVI on day 10. This trend is similar to the effect of adding powdered activated carbon to the HSAD systems of the OFMSW.[10] In general, if the TAN concentration exceeds 4000 mg/L, the AD system can be disrupted.[26] Reports suggest that the inhibition range of TAN and FAN for the OFMSW was 1200−8000 and 45−680 mg/L, respectively.[10] Notably, FAN has more toxicity than TAN because FAN can penetrate microbial cell membranes. Throughout the entire AD process, the FAN concentration range was 37−468.6 mg/L for all experimental groups, with expert for 685.4 mg/L for R-GAC on day 30. Therefore, the HSAD system of the OFMSW remained stable, as indicated by the VFA and FAN concentrations in the leachate.

3.3. Microbial Community Composition Analysis. In the AD system, bacteria and archaea functional microorganisms can play important roles, and the abundance of these microorganisms is closely related to the methane production performance.[34]

3.3.1. Bacterial Composition. The changes in the bacterial community are shown in Figure 4 at the phylum and genus levels. *Firmicutes*, *Bacteroidotas*, *Spirochaetota*, *Proteobacteria*, *synergistota*, and *Cloacimonadotas* were the dominant bacteria at the phylum levels (Figure 4(a)). These microbes can utilize the OFMSW to generate VFAs and H_2, especially easily biodegraded carbohydrates and proteins in the OFMSW.[35] The relative abundances of *Firmicutes* accounted for 56.3−68.4% of the total population, which is the highest of 68.4% in the R-(GAC + ZVI) group. *Firmicutes* play the role of maintaining system stability and are known for their acid-forming capabilities.[36] The high abundance of *Firmicutes* in R-(GAC + ZVI) indicated that this system has a strong buffering capacity after the addition of GAC and ZVI simultaneously. The relative abundance of *Bacteroidota* was 22.5 and 22%, without profound changes compared to the R-control (21.2%). Compared to the R-control, the relative abundances of *Spirochaetota* and *Proteobacteria* substantially increased from 7.4 to 11.8% and from 2.6 to 5.1% for R-GAC and R-ZVI, respectively.

At the genus level, a total of 27 bacterial sequences were identified with an abundance of >1%; norank_f__norank_o__norank_c__norank_p__*Firmicutes*, norank_f__norank_o__*MBA03*, *Fastidiosipila*, norank_f__*Rikenellaceae*, and *Sphaerochaeta* were the dominant genera (Figure 4(d)). The relative abundances of norank_f__norank_o__norank_c__norank_p__*Firmicutes* were 17.1−30.8% for different experiment groups. The highest relative abundance of norank_f__norank_o__norank_c__norank_p__*Firmicutes* was 30.8% for R-(GAC + ZVI), which was 71.4% higher than that of R-control. The genus norank_f__norank_o__norank_c__norank_p__*Firmicutes* is an unclassified anaerobic bacterium that belongs to the phylum *Firmicutes*.[37] The high abundance of norank_f__norank_o__norank_c__norank_p__*Firmicutes* in the GAC and ZVI addition groups suggested that norank_f__norank_o__norank_c__norank_p__*Firmicutes* played a crucial role in promoting the hydrolysis and acidification of the OFMSW into small molecules of VFAs and H_2 in HSAD systems. Furthermore, Qi et al. found Firmicutes as the dominant phylum in the solid-state anaerobic codigestion of sewage sludge and organic waste.[38] The norank_f__norank_o__*MBA03* can balance the system stability and produce VFAs within the entire methanogenic microbial community.[39] Additionally, *Fastidiosipila*, norank_f__*Rikenellaceae*, *Sphaerochaeta*, and *Fermentimonas* were the dominant genera after adding GAC and ZVI, with their relative abundances of 6.4−10.8, 6.2−9.8, 1.6−7.4, and 3.9−5.9%, considerably higher than that of the R-control. *Fastidiosipila* and *Fermentimonas* and norank_f__*Rikenellaceae* and *Sphaerochaeta* were the dominant genera for R-GAC and R-ZVI, respectively. *Fastidiosipila* can convert the OFMSW into VFAs and CO_2, which plays a critical role in the hydrolysis and acidification process.[40] Similarly, *Fermentimonas* can also use complex organic matter to produce VFAs, H_2, and CO_2.[22] After the addition of GAC, *Rikenellaceae* and *Sphaerochaeta* appeared higher in their relative abundances in the HSAD system for R-GAC and R-(GAC + ZVI) compared to the R-control. Moreover, *Rikenellaceae* and *Sphaerochaeta* were confirmed to possess DIET capabilities,[22] indicating an enhancement in the electron transfer capacity and methane production in the HSAD system after GAC addition in the HSAD system.

3.3.2. Archaeal Composition. At the archaea phylum level, *Halobacterota*, *Euryarchaeota*, and *Thermoplasmatota* were the

https://doi.org/10.1021/acsomega.3c06722
ACS Omega 2024, 9, 3401−3411

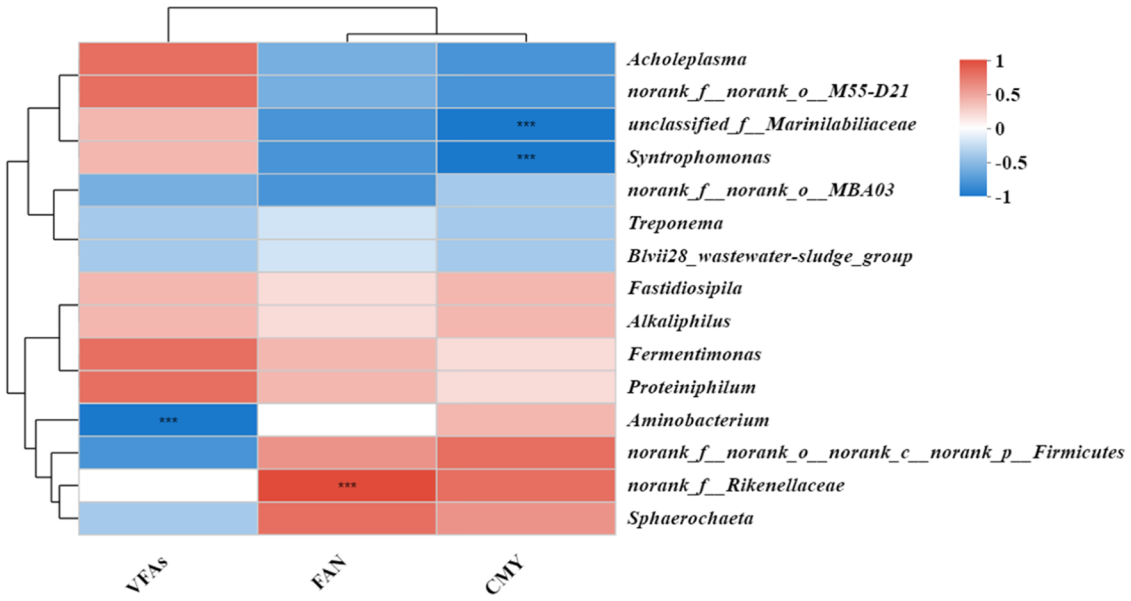

Figure 5. Correlation heatmap of VFAs, FAN, CMY, and bacteria.

major archaeal communities of these three phyla (Figure 4(b)), with relative abundances of 64.2−80.2, 17.7−32.5, and 2.0−6.9%, respectively. *Methanoculleus*, *Methanobacterium*, and *Methanosarcina* were the dominant genera at the genus levels (Figure 4(c)). The relative abundances of *Methanoculleus* were 63.6, 78.5, 57.0, and 60.9% for R-GAC, R-ZVI, R-(GAC + ZVI), and R-control, respectively. *Methanoculleus* is found in treating food waste-recycling wastewater process.[41] Additionally, the relative abundance of *Methanobacterium* was 15.9−29.9%, which was the second most abundant genus at the archaea genus level. *Methanobacterium* is a hydrogenotrophic methanogen responsible for converting H_2/CO_2 to methane.[40] In the R-control group, the relative abundance of *Methanoculleus* and *Methanobacterium* accounted for 90.8% of the total archaeal abundance, with similar percentages in the R-GAC and R-(GAC + ZVI) at 83.7 and 79.0%, respectively. Furthermore, the relative abundance of *Methanosarcina* was 10.6% for R-(GAC + ZVI), which was far higher than those of R-GAC (4.7%), R-ZVI (0.5%), and the R-control (1.1%). *Methanosarcina*, an acetoclastic methanogen, can tolerate high ammonia concentrations and convert diverse substrates, such as acetate and H_2/CO_2 to methane,[42] and can exchange electrons in the extracellular to achieve DIET.[43] These findings show that methane production in the AD process after GAC and ZVI addition primarily originates from acetic acid and H_2/CO_2. The CMY of R-(GAC + ZVI) was higher than those of the other groups, which can be attributed to the combined action of *Methanoculleus*, *Methanobacterium*, and *Methanosarcina*.

3.3.3. Correlations between AD Parameters and Bacteria. The correlation between the bacterial community and VFAs, TAN, and CMY of the OFMSW is shown at the genus level (Figure 5). *Acholeplasma* (R = 0.8), norank_f__norank_o_*M55-D21* (R = 0.8), *Fermentimonas* (R = 0.8), and *Proteiniphilum* (R = 0.8) showed a positive correlation with VFAs. Conversely, *Aminobacterium* (R = −1***) and norank_f__norank_o__norank_c__norank_p__*Firmicutes* (R = −0.8) exhibited a negative correlation with VFAs. Unclassified_f__*marinilabiliaceae* (R = −1***) and *Syntrophomonas* (R = −1***) displayed a strong negative correlation with the CMY. However, norank_f__norank_o__norank_c__norank_p__*Firmicutes* (R = 0.8 and R = 0.6) and norank_f__*Rikenellaceae* (R = 0.8 and R = 1.0***) exhibited a positive relation with the CMY and FAN. This further indicated that norank_f__norank_o__norank_c__norank_p__*Firmicutes* and norank_f__*Rikenellaceae* play crucial roles during the hydrolysis and acidogenesis processes and convert VFAs to methane. This observation is consistent with the changes in the bacterial microbial community structure and methanogenic properties of the different systems described previously.

4. CONCLUSIONS

In the HSAD system, the simultaneous addition of GAC and ZVI increases the methane yield in the OFMSW, although it does not considerably affect the AD period compared to single GAC, ZVI, and R-control additions. The maximum CMY of 343.0 mL/gVS was obtained in R-(GAC + ZVI), which was 57.1% higher than that of the R-control. Bacteria of norank_f__norank_o__norank_c__norank_p__*Firmicutes*, norank_f__norank_o__*MBA03*, *Fastidiosipila*, norank_f__*Rikenellaceae*, and *Sphaerochaeta* and archaea of *Methanoculleus*, *Methanobacterium*, and *Methanosarcina* were the dominant genera at the genus levels. After the addition of GAC and ZVI, the electron transfer capacity of the HSAD system was enhanced, thereby promoting methane production.

AUTHOR INFORMATION

Corresponding Authors

Hairong Yuan − *State Key Laboratory of Chemical Resource Engineering, Department of Environmental Science and Engineering, Beijing University of Chemical Technology, Beijing 100029, P. R. China;* orcid.org/0000-0003-1831-3104; Email: yuanhairong75@163.com

Xiujin Li − *State Key Laboratory of Chemical Resource Engineering, Department of Environmental Science and Engineering, Beijing University of Chemical Technology, Beijing 100029, P. R. China;* orcid.org/0000-0003-4484-2050; Phone: +86-010-6443-2281; Email: xjli@mail.buct.edu.cn

https://doi.org/10.1021/acsomega.3c06722
ACS Omega 2024, 9, 3401−3411

Authors

Hongfei Zhang − *State Key Laboratory of Chemical Resource Engineering, Department of Environmental Science and Engineering, Beijing University of Chemical Technology, Beijing 100029, P. R. China; Cscec Scimee Science and Technology Limited Liability Company, Chengdu 610045, P. R. China*

Xiaoyu Zuo − *State Key Laboratory of Chemical Resource Engineering, Department of Environmental Science and Engineering, Beijing University of Chemical Technology, Beijing 100029, P. R. China;* orcid.org/0000-0002-8250-4311

Liang Zhang − *State Key Laboratory of Chemical Resource Engineering, Department of Environmental Science and Engineering, Beijing University of Chemical Technology, Beijing 100029, P. R. China*

Complete contact information is available at: https://pubs.acs.org/10.1021/acsomega.3c06722

Notes

The authors declare no competing financial interest.

■ ACKNOWLEDGMENTS

The authors are grateful for the fund supports from the Fundamental Research Funds for the Central Universities (JD2326).

■ REFERENCES

(1) Wang, Z.; Hu, Y.; Wang, S.; Wu, G.; Zhan, X. A critical review on dry anaerobic digestion of organic waste: Characteristics, operational conditions, and improvement strategies. *Renewable Sustainable Energy. Rev.* **2023**, *176*, No. 113208.

(2) MEE. *Annual Report on the Prevention and Control of Environmental Pollution by Large and Medium-Sized Municipal Solid Waste in China 2022*, Ministry of Ecology and Environment of the People's Republic of China, BeiJing2022.

(3) Mlaik, N.; Karray, F.; Sayadi, S.; Feki, F.; Khoufi, S. Semi-continuous anaerobic digestion of the organic fraction of municipal solid waste: digester performance and microbial population dynamics. *J. Environ. Chem. Eng.* **2022**, *10*, No. 107941.

(4) Ibarra-Esparza, F. E.; González-López, M. E.; Ibarra-Esparza, J.; Lara-Topete, G. O.; Senés-Guerrero, C.; Cansdale, A.; Forrester, S.; Chong, J. P. J.; Gradilla-Hernández, M. S. Implementation of anaerobic digestion for valorizing the organic fraction of municipal solid waste in developing countries: Technical insights from a systematic review. *J. Environ. Manage.* **2023**, *347*, No. 118993.

(5) Silva-Martínez, R. D.; Sanches-Pereira, A.; Ornelas-Ferreira, B.; Carneiro-Pinheiro, B.; Coelho, S. T. High solid and wet anaerobic digestion technologies for the treatment of the organic fraction of municipal solid wastes and food wastes: A comparative case study in Brazil. *Bioresour. Technol. Rep.* **2023**, *21*, No. 101306, DOI: 10.1016/j.biteb.2022.101306.

(6) Wu, L.; Jin, T.; Chen, H.; Shen, Z.; Zhou, Y. Conductive materials as fantastic toolkits to stimulate direct interspecies electron transfer in anaerobic digestion: new insights into methanogenesis contribution, characterization technology, and downstream treatment. *J. Environ. Manage.* **2023**, *326*, No. 116732.

(7) Alam, M.; Dhar, B. R. Boosting thermophilic anaerobic digestion with conductive materials: Current outlook and future prospects. *Chemosphere* **2023**, *343*, No. 140175.

(8) Kutlar, F. E.; Tunca, B.; Yilmazel, Y. D. Carbon-based conductive materials enhance biomethane recovery from organic wastes: A review of the impacts on anaerobic treatment. *Chemosphere* **2022**, *290*, No. 133247.

(9) Feng, L.; He, S.; Gao, Z.; Zhao, W.; Jiang, J.; Zhao, Q.; Wei, L. Mechanisms, performance, and the impact on microbial structure of direct interspecies electron transfer for enhancing anaerobic digestion-A review. *Sci. Total Environ.* **2023**, *862*, No. 160813, DOI: 10.1016/j.scitotenv.2022.160813.

(10) Dastyar, W.; Azizi, S. M. M.; Meshref, M. N. A.; Dhar, B. R. Powdered activated carbon amendment in percolate tank enhances high-solids anaerobic digestion of organic fraction of municipal solid waste. *Process Saf. Environ. Prot.* **2021**, *151*, 63−70.

(11) Tiwari, S. B.; Dubey, M.; Ahmed, B.; Gahlot, P.; Khan, A. A.; Rajpal, A.; Kazmi, A. A.; Tyagi, V. K. Carbon-based conductive materials facilitated anaerobic co-digestion of agro waste under thermophilic conditions. *Waste Manage.* **2021**, *124*, 17−25.

(12) Xiao, Y.; Yang, H.; Yang, H.; Wang, H.; Zheng, D.; Liu, Y.; Pu, X.; Deng, L. Improved biogas production of dry anaerobic digestion of swine manure. *Bioresour. Technol.* **2019**, *294*, No. 122188.

(13) Dang, Y.; Sun, D.; Woodard, T. L.; Wang, L.-Y.; Nevin, K. P.; Holmes, D. E. Stimulation of the anaerobic digestion of the dry organic fraction of municipal solid waste (OFMSW) with carbon-based conductive materials. *Bioresour. Technol.* **2017**, *238*, 30−38.

(14) Xiao, L.; Liu, J.; Kumar, P. S.; Zhou, M.; Yu, J.; Lichtfouse, E. Enhanced methane production by granular activated carbon: A review. *Fuel* **2022**, *320*, No. 123903.

(15) Xu, W.; He, X.; Wang, C.; Zhao, Z. Effect of granular activated carbon adsorption and size of microbial aggregates in inoculum on stimulating direct interspecies electron transfer during anaerobic digestion of fat, oil, and grease. *Bioresour. Technol.* **2023**, *368*, No. 128289.

(16) Wang, P.; Li, X.; Li, Y.; Su, Y.; Wu, D.; Xie, B. Enhanced anaerobic digestion performance of food waste by zero-valent iron and iron oxides nanoparticles: Comparative analyses of microbial community and metabolism. *Bioresour. Technol.* **2023**, *371*, No. 128633.

(17) Liang, J.; Luo, L.; Li, D.; Varjani, S.; Xu, Y.; Wong, J. W. Promoting anaerobic co-digestion of sewage sludge and food waste with different types of conductive materials: Performance, stability, and underlying mechanism. *Bioresour. Technol.* **2021**, *337*, No. 125384.

(18) Kassab, G.; Khater, D.; Odeh, F.; Shatanawi, K.; Halalsheh, M.; Arafah, M.; van Lier, J. B. Impact of nanoscale magnetite and zero valent iron on the batch-wise anaerobic co-digestion of food waste and waste-activated sludge. *Water* **2020**, *12* (5), No. 1283, DOI: 10.3390/w12051283.

(19) Zhao, Z.; Zhang, Y.; Li, Y.; Quan, X.; Zhao, Z. Comparing the mechanisms of ZVI and Fe_3O_4 for promoting waste-activated sludge digestion. *Water Res.* **2018**, *144*, 126−133.

(20) Zhang, D.; Wei, Y.; Wu, S.; Zhou, L. Rapid initiation of methanogenesis in the anaerobic digestion of food waste by acclimatizing sludge with sulfidated nanoscale zerovalent iron. *Bioresour. Technol.* **2021**, *341*, No. 125805.

(21) Niu, J.; Kong, X.; Che, Q.; Li, Q.; Yuan, J.; Liu, J.; Zhang, Y. Insights into the effects of micro and nanoscale Fe0 on elimination of excessive acidification during anaerobic digestion of the organic fraction of municipal solid waste: Similarities and differences in reactor performance and syntrophic metabolism. *Fuel* **2022**, *320*, No. 123923.

(22) Guan, R.; Yuan, H.; Zhang, L.; Zuo, X.; Li, X. Combined pretreatment using CaO and liquid fraction of digestate of rice straw: Anaerobic digestion performance and electron transfer. *Chin. J. Chem. Eng.* **2021**, *36*, 223−232.

(23) Wei, Y.; Bao, R.; Guan, R.; Li, X.; Zuo, X.; Yuan, H. Solid-State Co-digestion of Food Waste and Highland Barley Straw: Effect of Inoculum-Substrate Ratio on the Performance and Microbial Community Structure. *Waste Biomass Valorization* **2023**, *36*, 223−232, DOI: 10.1007/s12649-023-02271-9.

(24) Jiang, Y.; McAdam, E.; Zhang, Y.; Heaven, S.; Banks, C.; Longhurst, P. Ammonia inhibition and toxicity in anaerobic digestion: A critical review. *J. Water Process Eng.* **2019**, *32*, No. 100899.

(25) Guan, R.; Gu, J.; Wachemo, A. C.; Yuan, H.; Li, X. Novel insights into anaerobic digestion of rice straw using combined pretreatment with CaO and the liquid fraction of digestate: anaerobic

digestion performance and kinetic analysis. *Energy Fuels* **2020**, *34*, 1119−1130.
(26) Wei, Y.; Gao, Y.; Yuan, H.; Chang, Y.; Li, X. Effects of organic loading rate and pretreatments on digestion performance of corn stover and chicken manure in completely stirred tank reactor (CSTR). *Sci. Total Environ.* **2022**, *815*, No. 152499.
(27) Dai, C.; Yang, L.; Wang, J.; Li, D.; Zhang, Y.; Zhou, X. Enhancing anaerobic digestion of pharmaceutical industries wastewater with the composite addition of zero valent iron (ZVI) and granular activated carbon (GAC). *Bioresour. Technol.* **2022**, *346*, No. 126566.
(28) Zhang, S.; Ma, X.; Xie, D.; Guan, W.; Yang, M.; Zhao, P.; Gao, M.; Wang, Q.; Wu, C. Adding activated carbon to the system with added zero-valent iron further improves anaerobic digestion performance by alleviating ammonia inhibition and promoting DIET. *J. Environ. Chem. Eng.* **2021**, *9*, No. 106616.
(29) Yuan, T.; Shi, X.; Sun, R.; Ko, J. H.; Xu, Q. MEE Simultaneous addition of biochar and zero-valent iron to improve food waste anaerobic digestion. *J. Cleaner Prod.* **2021**, *278*, No. 123627.
(30) Yellezuome, D.; Zhu, X.; Liu, X.; Liu, X.; Liu, R.; Wang, Z.; Li, Y.; Sun, C.; Abd-Alla, M. H.; Rasmey, A.-H. M. Integration of two-stage anaerobic digestion process with in situ biogas upgrading. *Bioresour. Technol.* **2023**, *369*, No. 128475.
(31) Wei, Y.; Wachemo, A. C.; Yuan, H.; Li, X. Enhanced hydrolysis and acidification strategy for efficient co-digestion of pretreated corn stover with chicken manure: Digestion performance and microbial community structure. *Sci. Total Environ.* **2020**, *720*, No. 137401.
(32) Ryue, J.; Lin, L.; Liu, Y.; Lu, W.; McCartney, D.; Dhar, B. R. Comparative effects of GAC addition on methane productivity and microbial community in mesophilic and thermophilic anaerobic digestion of food waste. *Biochem. Eng. J.* **2019**, *146*, 79−87.
(33) Zhu, R.; He, L.; Li, Q.; Huang, T.; Gao, M.; Jiang, Q.; Liu, J.; Cai, A.; Shi, D.; Gu, L.; He, Q. Mechanism study of improving anaerobic co-digestion performance of waste activated sludge and food waste by Fe_3O_4. *J. Environ. Manage.* **2021**, *300*, No. 113745.
(34) Hu, J.; Li, Z.; Tao, W. How dose calcium hypochlorite promote the methane production from sludge anaerobic digestion: A mechanism study from enhanced biodegradability of recalcitrant substances. *J. Water Process Eng.* **2022**, *50*, No. 103268.
(35) Hu, J.; Li, Z.; Tao, W. Calcium Hypochlorite Promotes Dark Fermentative Hydrogen Production from Waste Activated Sludge. *ACS Sustainable Chem. Eng.* **2022**, *10*, 2509−2521.
(36) Shi, Z.; Zhang, L.; Yuan, H.; Li, X.; Chang, Y.; Zuo, X. Oyster shells improve anaerobic dark fermentation performances of food waste: Hydrogen production, acidification performances, and microbial community characteristics. *Bioresour. Technol.* **2021**, *335*, No. 125268.
(37) Xu, L.; Wang, Y.; Xuan, L.; Mei, H.; He, C.; Yang, J.; Wang, W. New attempts on acidic anaerobic digestion of poly (butylene adipate-co-terephthalate) wastewater in upflow anaerobic sludge blanket reactor. *J. Hazard. Mater.* **2024**, *461*, No. 132586.
(38) Qi, C.; Cao, D.; Gao, X.; Jia, S.; Yin, R.; Nghiem, L. D.; Li, G.; Luo, W. Optimising organic composition of feedstock to improve microbial dynamics and symbiosis to advance solid-state anaerobic co-digestion of sewage sludge and organic waste. *Appl. Energy* **2023**, *351*, No. 121857.
(39) Liu, X.; Zhu, X.; Yellezuome, D.; Liu, R.; Liu, X.; Sun, C.; Abd-Alla, M. H.; Rasmey, A.-H. M. Effects of adding Thermoanaerobacterium thermosaccharolyticum in the hydrogen production stage of a two-stage anaerobic digestion system on hydrogen-methane production and microbial communities. *Fuel* **2023**, *342*, No. 127831.
(40) Bao, R.; Wei, Y.; Guan, R.; Li, X.; Lu, X.; Rong, S.; Zuo, X.; Yuan, H. High-solids anaerobic co-digestion performances and microbial community dynamics in co-digestion of different mixing ratios with food waste and highland barley straw. *Energy* **2023**, *262*, No. 125529.
(41) Kim, S. I.; Chairattanawat, C.; Kim, E.; Hwang, S. Shift in methanogenic community in protein degradation using different inocula. *Bioresour. Technol.* **2021**, *333*, No. 125145.
(42) Jannat, M. A. H.; Park, S. H.; Chairattanawat, C.; Yulisa, A.; wang, S. H. Effect of different microbial seeds on batch anaerobic digestion of fish waste. *Bioresour. Technol.* **2022**, *349*, No. 126834, DOI: 10.1016/j.biortech.2022.126834.
(43) Lin, R.; Cheng, J.; Zhang, J.; Zhou, J.; Cen, K.; Murphy, J. D. Boosting biomethane yield and production rate with graphene: The potential of direct interspecies electron transfer in anaerobic digestion. *Bioresour. Technol.* **2017**, *239*, 345−352.

https://doi.org/10.1021/acsomega.3c06722
ACS Omega 2024, 9, 3401−3411